




Quantum fluctuations in multiphoton Compton scattering

Dejia Dai  and Libin Fu *

Graduate School, China Academy of Engineering Physics, Beijing 100193, China

 (Received 28 July 2021; revised 31 October 2021; accepted 16 December 2021; published 3 January 2022)

We propose a method to study the interaction of a single-mode laser beam (as an external field) containing a finite number of photons with a free electron. In particular, we give some numerical results of how the photon number $l_{k,\varepsilon}$ affects the differential scattering cross section when the initial state of an external field is a Fock state $|l_{k,\varepsilon}\rangle$. Besides, for arbitrarily polarized light, we prove that our model will return to the semiclassical theory as $l_{k,\varepsilon} \rightarrow \infty$.

DOI: [10.1103/PhysRevA.105.013101](https://doi.org/10.1103/PhysRevA.105.013101)

I. INTRODUCTION

Strong-field dynamics is a hot research topic and widely exists in various quantum systems [1–4]. The classical [5–8] and semiclassical [9–14] theoretical studies on multiphoton Compton scattering in the past are satisfactory, and the leap-forward development of laser technology [15] proves this point experimentally [16–22]. It should be pointed out that these experiments and theories imply that the initial photon number $l_{k,\varepsilon}$ of the external field is sufficiently large ($l_{k,\varepsilon} \rightarrow \infty$) so that the laser can be treated as a fixed classical background field [1, 13]. This processing method is also applicable to other strong-field systems, such as strong-field ionization [23–26] and harmonic generation [27, 28]. However, when $l_{k,\varepsilon}$ is finite or even small in magnitude, the depletion of external fields [29–31] must be considered. In this case, how to deal with the processes of light-matter interaction is a problem worthy of attention. In particular, for multiphoton Compton scattering, it is meaningful to investigate the effect of $l_{k,\varepsilon}$ on some physical quantities (especially the on differential scattering cross section).

It is a well-known fact that the motion of free electrons in a classical plane-wave electromagnetic-field $A_{k,\varepsilon}^{cl}(x)$ is usually described by Volkov states [32]. Utilizing the boundary conditions $A_{k,\varepsilon}^{cl}(\mathbf{r}, t \rightarrow \pm\infty) = 0$ [2], Volkov states will transform into free states when $t \rightarrow \pm\infty$. Based on the Furry picture [33], the incident and outgoing states of electrons can be treated as Volkov states in the semiclassical theory [10–14] of multiphoton Compton scattering. Obviously, the Volkov state involving the classical field does not reflect the information of the photon number in the radiation field. Here, Fried and Eberly [34] once proposed to use the full quantum electrodynamics (QED) method of summing Feynman diagrams to deal with multiphoton Compton scattering. This method could be used to calculate the corresponding scattering cross section for a given $l_{k,\varepsilon}$, although their work needed some refinement [35, 36]. In addition, Begrou and Sarro [37] also studied analogous problems by using a quantized background field.

In this paper, starting from the Dirac equation, we try to reexamine the multiphoton Compton scattering process from the perspective of QED. By quantizing the background field, the Volkov state involving the quantum field was obtained [37–39], and it can accurately describe the photon number of the background field. Inspired by this, we numerically describe the quantum fluctuations of the differential scattering cross section with $l_{k,\varepsilon}$ in the multiphoton Compton scattering process. The results show that $l_{k,\varepsilon}$ will affect the differential scattering cross section to some extent. Meanwhile, we also prove that our results will return to the semiclassical results [10] when $l_{k,\varepsilon} \rightarrow \infty$.

The paper is organized as follows. In Sec. II, we describe the calculation process of the differential scattering cross section in detail and give a theoretical proof in the classical limit. Our numerical results and conclusions are presented in Secs. III and IV, respectively. If there is no special declaration, natural units (n.u.) with $\hbar = c = \epsilon_0 = 1$ are employed throughout this paper. ϵ_0 is the permittivity of vacuum. \not{a} is Feynman slash notation, representing $g_{\mu\nu}\gamma^\mu a^\nu$ ($\mu, \nu = 0-3$). γ^μ s are the 4×4 Dirac matrices and the space-time metric $g^{\mu\nu} = \text{diag}(1, -1, -1, -1)$. In addition, we abbreviate the multiplication of two four-vectors $a_\mu b^\mu$ as $a \cdot b$.

II. MODEL

A. S-matrix element for multiphoton Compton scattering

The electronic wave-function $|\psi(x)\rangle$ in the electromagnetic field satisfies the Dirac equation,

$$i \frac{\partial}{\partial t} |\psi(x)\rangle = \{\gamma^0 \boldsymbol{\gamma} \cdot [-i\nabla + e\mathbf{A}(x)] + \gamma^0 m_e\} |\psi(x)\rangle, \quad (1)$$

where $-e$ and m_e represent the charge and rest mass of the electron, respectively. Furthermore, the Coulomb gauge is used for $A(x)$, that is, $A(x) = [0, \mathbf{A}(x)]$ and $\nabla \cdot \mathbf{A}(x) = 0$. Considering the collision between an electron and a single-mode laser beam containing $l_{k,\varepsilon}$ photons, we are more concerned about that a single photon scattered from the laser beam (see Fig. 1). The corresponding transition-matrix

*lbfu@gscap.ac.cn

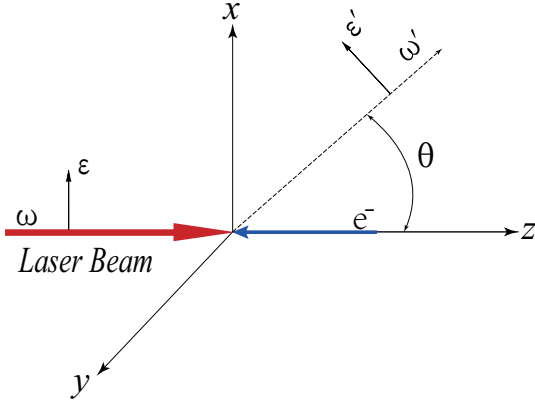


FIG. 1. The schematic of multiphoton Compton scattering. The laser beam contains $l_{k,\varepsilon}$ photons. After the laser beam interacts with an electron, a photon of frequency ω' is scattered from the laser beam. The parameters ω (ω') and ε (ε') are the frequency and the polarization vector of the laser beam (the scattered photon), respectively.

element is expressed as

$$S_{fi} = \langle \phi_{\text{out}}(\mathbf{r}, t_f) | U(t_f, t_i) | \phi_{\text{in}}(\mathbf{r}, t_i) \rangle. \quad (2)$$

Here $|\phi_{\text{in}}(\mathbf{r}, t_i)\rangle$ and $|\phi_{\text{out}}(\mathbf{r}, t_f)\rangle$ are the wave functions of the initial and final electrons, respectively, and $U(t_f, t_i)$ is the time-evolution operator.

In order to get $U(t_f, t_i)$, we decompose $\mathbf{A}(x)$ into

$$\mathbf{A}(x) = \mathbf{A}_{k,\varepsilon}(x) + \sum_{\varepsilon'} \sum_{k' \neq k} \mathbf{A}_{k',\varepsilon'}(x), \quad (3)$$

where $k = (\omega, \mathbf{k})$ is the four-momentum of the single photon in the laser beam, and $k' = (\omega', \mathbf{k}')$ is the four-momentum of the scattered photon; $\varepsilon' = (0, \mathbf{\varepsilon}')$ and $\mathbf{k}' \cdot \mathbf{\varepsilon}' = 0$. Let us make

$$\begin{aligned} H_0 &= \gamma^0 \boldsymbol{\gamma} \cdot [-i\nabla + e\mathbf{A}_{k,\varepsilon}(x)] + \gamma^0 m_e, \\ H' &= \sum_{\varepsilon'} \sum_{k' \neq k} e\gamma^0 \boldsymbol{\gamma} \cdot \mathbf{A}_{k',\varepsilon'}(x), \end{aligned} \quad (4)$$

and define the time-evolution operator $U_0(t, t_i)$, which satisfies the following relation:

$$i \frac{\partial}{\partial t} U_0(t, t_i) = H_0 U_0(t, t_i). \quad (5)$$

Then we obtain

$$U(t_f, t_i) = U_0(t_f, t_i) - i \int_{t_i}^{t_f} U_0(t_f, t) H' U(t, t_i) dt. \quad (6)$$

If only the first-order process is considered, we have

$$U(t_f, t_i) = U_0(t_f, t_i) - i \int_{t_i}^{t_f} U_0(t_f, t) H' U_0(t, t_i) dt. \quad (7)$$

Now, we quantize both $\mathbf{A}_{k,\varepsilon}(x)$ and $\mathbf{A}_{k',\varepsilon'}(x)$, that is,

$$\begin{aligned} \mathbf{A}_{k,\varepsilon}(x) &= g(\varepsilon a_{k,\varepsilon} e^{-ik \cdot x} + \text{H.c.}) \\ \mathbf{A}_{k',\varepsilon'}(x) &= \sqrt{\frac{1}{2\omega'V}} (\varepsilon' a_{k',\varepsilon'} e^{-ik' \cdot x} + \text{H.c.}), \end{aligned} \quad (8)$$

where $g = (2\omega V)^{-1/2}$ and V is the normalized volume of the light field; $\varepsilon = [0, \cos(\xi/2), i \sin(\xi/2), 0]$ and ξ is the polarization parameter of the incident laser. $a_{k,\varepsilon}$ ($a_{k',\varepsilon}'$) is the annihilation operator for the incident (scattered) photon. When $t_i \rightarrow -\infty$ and $t_f \rightarrow +\infty$, electrons have no interaction with the light field, and they should be described by free states. Therefore, the boundary conditions are given by

$$\begin{aligned} \phi_{\text{in}}(\mathbf{r}, t_i \rightarrow -\infty) &= e^{-iE_p t_i} \langle \mathbf{r} | p \rangle \otimes |l_{k,\varepsilon}\rangle \otimes |0_{k',\varepsilon}'\rangle, \\ \phi_{\text{out}}(\mathbf{r}, t_f \rightarrow +\infty) &= e^{-iE_{p'} t_f} \langle \mathbf{r} | p' \rangle \otimes |n_{k,\varepsilon}\rangle \otimes |1_{k',\varepsilon}'\rangle. \end{aligned} \quad (9)$$

Here $p = (E_p, \mathbf{p})$ and $p' = (E_{p'}, \mathbf{p}')$ are the four-momentum of the initial and final electrons, respectively. $l_{k,\varepsilon}$ and $n_{k,\varepsilon}$ are the number of photons before and after scattering in the laser beam. Substituting Eqs. (7) and (9) into Eq. (2), we obtain

$$S_{fi} = -i \int_{-\infty}^{+\infty} \langle \psi_{p'}(\mathbf{r}, t) | \langle 1_{k',\varepsilon}' | H' | 0_{k',\varepsilon}' \rangle | \psi_p(\mathbf{r}, t) \rangle dt, \quad (10)$$

where

$$\begin{aligned} |\psi_p(\mathbf{r}, t)\rangle &= \lim_{t_i \rightarrow -\infty} U_0(t, t_i) \langle \mathbf{r} | p \rangle \otimes |l_{k,\varepsilon}\rangle e^{-iE_p t_i}, \\ |\psi_{p'}(\mathbf{r}, t)\rangle &= \lim_{t_f \rightarrow +\infty} U_0(t, t_f) \langle \mathbf{r} | p' \rangle \otimes |n_{k,\varepsilon}\rangle e^{-iE_{p'} t_f}. \end{aligned} \quad (11)$$

According to Eq. (5), $|\psi_p(\mathbf{r}, t)\rangle$ and $|\psi_{p'}(\mathbf{r}, t)\rangle$ are both the solutions of the following equation:

$$i \frac{\partial}{\partial t} |\psi(x)\rangle = H_0 |\psi(x)\rangle. \quad (12)$$

This equation has the following form solution [39,40]:

$$\begin{aligned} \psi_{qn'k,\varepsilon s}^V(x) &= \exp(ik \cdot x \hat{N} - iqx - iZ_{n'k,\varepsilon s} k \cdot x) \\ &\times \frac{1}{\sqrt{J_{qn'k,\varepsilon s} V}} \left(1 - \frac{e\mathcal{A}}{2kq} \right) D_q^\dagger S_q |n'_{k,\varepsilon}\rangle \mathcal{P}(\mathcal{S} + s)v, \end{aligned} \quad (13)$$

where

$$\begin{aligned} \hat{N} &= \frac{1}{2}(a_{k,\varepsilon} a_{k,\varepsilon}^\dagger + a_{k,\varepsilon}^\dagger a_{k,\varepsilon}), \\ Z_{n'k,\varepsilon s} &= (k \cdot q)^{-1} [Z(n'_{k,\varepsilon} + \frac{1}{2}) - e^2 g^2 Z^{-1} |q \cdot \varepsilon \cosh \chi \\ &\quad + q \cdot \varepsilon^* \sinh \chi|^2 + \frac{1}{2} e^2 g^2 s], \\ Z &= [(k \cdot q + e^2 g^2)^2 - e^4 g^4 \cos^2 \xi]^{1/2}, \\ \tanh 2\chi &= -e^2 g^2 \cos \xi / (k \cdot q + e^2 g^2). \end{aligned} \quad (14)$$

q is the four-momentum of the free electron and satisfies $q^2 - m_e^2 = 0$; $s = \pm \sin \xi$; $\mathcal{A} = g(\varepsilon a_{k,\varepsilon} + \varepsilon^* a_{k,\varepsilon}^\dagger)$. The expressions of operators D_q^\dagger and S_q are as follows:

$$\begin{aligned} D_q^\dagger &= \exp(\delta a_{k,\varepsilon}^\dagger - \delta^* a_{k,\varepsilon}), \\ S_q &= \exp \left[\frac{\chi}{2} (a_{k,\varepsilon}^\dagger a_{k,\varepsilon}^\dagger - a_{k,\varepsilon} a_{k,\varepsilon}) \right], \\ \delta &= egq \cdot (\varepsilon \sinh 2\chi + \varepsilon^* \cosh 2\chi) / Z. \end{aligned} \quad (15)$$

The bispinor $\mathcal{P}(\mathcal{S} + s)v$ satisfies the stationary state Dirac equation of free electrons, and it is discussed in detail in Appendix A. For convenience, let us mark it as u_{qs} . Moreover,

$J_{qn'_{k,\varepsilon}S}$ is the normalization coefficient,

$$J_{qn'_{k,\varepsilon}S} = \frac{1}{m_e} [q^0 + \omega Z_{n'_{k,\varepsilon}S} - |\delta|^2 \omega - \omega(n'_{k,\varepsilon} + 1/2) \cosh 2\chi]. \quad (16)$$

Hence, we can treat $|\psi_p(\mathbf{r}, t)\rangle$ and $|\psi_{p'}(\mathbf{r}, t)\rangle$ as

$$\begin{aligned} |\psi_p(\mathbf{r}, t)\rangle &= \psi_{l_{k,\varepsilon}pS}^V(x), \\ |\psi_{p'}(\mathbf{r}, t)\rangle &= \psi_{n_{k,\varepsilon}p'S'}^V(x). \end{aligned} \quad (17)$$

Furthermore, the boundary of $\psi_{qn'_{k,\varepsilon}S}^V(x)$ needs some refinement, and we will discuss it in Appendix B.

We now return to Eq. (10), and there is

$$\langle 1_{k',\varepsilon'} | H' | 0_{k',\varepsilon'} \rangle = -\sqrt{\frac{e^2}{2\omega'V}} \gamma^0 \not{\epsilon}' e^{ik' \cdot x}, \quad (18)$$

Substituting Eqs. (13), (17), and (18) into Eq. (10), we obtain

$$S_{fi} = N_{fi} M_N \delta(p' + Z_{n_{k,\varepsilon}S'} k + k' - p - Z_{l_{k,\varepsilon}S} k), \quad (19)$$

where

$$\begin{aligned} N_{fi} &= i \frac{(2\pi)^4}{V \sqrt{J_{p'n_{k,\varepsilon}S'} J_{pl_{k,\varepsilon}S}}} \sqrt{\frac{e^2}{2\omega'V}}, \\ M_N &= \bar{u}_{p'S'} \langle n_{k,\varepsilon} | S_{p'}^\dagger D_{p'} \left[1 - \frac{e \not{\epsilon}' k}{2k \cdot p'} \right] \not{\epsilon}' \\ &\quad \times \left[1 - \frac{e k \not{\epsilon}}{2k \cdot p} \right] D_p^\dagger S_p | l_{k,\varepsilon} \rangle u_{pS}, \\ N &= l_{k,\varepsilon} - n_{k,\varepsilon}, \\ \bar{u}_{p'S'} &= u_{p'S'}^\dagger \gamma^0. \end{aligned} \quad (20)$$

The δ function in Eq. (19) reflects the energy-momentum conservation of the whole scattering system. Let

$$\begin{aligned} q_1 &= p + Z_{l_{k,\varepsilon}S} k - (l_{k,\varepsilon} + \frac{1}{2})k, \\ q_2 &= p' + Z_{n_{k,\varepsilon}S'} k - (n_{k,\varepsilon} + \frac{1}{2})k. \end{aligned} \quad (21)$$

Then, the energy-momentum conservation equation becomes

$$q_1 + Nk = q_2 + k', \quad (22)$$

and its form is completely consistent with the corresponding semiclassical equation [10]. In fact, when $l_{k,\varepsilon} \rightarrow \infty$, q_1 and q_2 will reduce into the ‘‘effective’’ four-momentum [2] of electrons in the external field [39]. Moreover, Eq. (22) shows that N is exactly the difference of the photon number before and after scattering in the light field $A_{k,\varepsilon}(x)$.

Correspondingly, the transition rate is given by

$$\begin{aligned} w_N &= \lim_{T \rightarrow \infty} \frac{1}{4} \sum_{s,s'} \sum_{\varepsilon,\varepsilon'} \sum_{k'} \sum_{p'} \frac{|S_{fi}|^2}{T} \\ &= \int d\Omega_{k'} \sum_{s,s'} \sum_{\varepsilon,\varepsilon'} \frac{e^2 \omega'}{32\pi^2 \sqrt{J_{p'n_{k,\varepsilon}S'} J_{pl_{k,\varepsilon}S}}} |M_N|^2, \end{aligned} \quad (23)$$

where 1/4 comes from averaging the electron spin and photon polarization in the initial state; $\mathbf{k}' = \omega'(\sin \theta \cos \varphi, \sin \theta \sin \varphi, \cos \theta)$; θ and φ are the azimuth

angles of \mathbf{k}' ; ω' is determined by Eq. (22). In addition, the photon number flux density can be written as

$$j_{\text{in}} = \frac{l_{k,\varepsilon}}{V}. \quad (24)$$

Thus, we can obtain the differential scattering cross section,

$$\frac{d\sigma_N}{d\Omega_{k'}} = \sum_{s,s'} \sum_{\varepsilon,\varepsilon'} \frac{e^2 \omega'}{32\pi^2 J_{p'n_{k,\varepsilon}S'} J_{pl_{k,\varepsilon}S} j_{\text{in}}} |M_N|^2. \quad (25)$$

Now, we could numerically compute the scattering cross section corresponding to given $l_{k,\varepsilon}$ and $n_{k,\varepsilon}$ with the help of Eqs. (20) and (25). The main steps of the numerical scheme are roughly as follows. First, when the initial parameters $p, k, l_{k,\varepsilon}, n_{k,\varepsilon}, s, s', \varepsilon, \varepsilon', \theta, \varphi$, and I are given, we can obtain the parameters ω' and p' through the energy-momentum conservation [see the δ function in Eq. (19)]. Second, we can express the operator $a_{k,\varepsilon}$ as a square matrix in the Fock representation. Naturally, we must truncate the dimension of the matrix. Similarly, the Fock states $|l_{k,\varepsilon}\rangle$ and $|n_{k,\varepsilon}\rangle$ can also be expanded into the column matrices with the same dimension as $a_{k,\varepsilon}$. Finally, Eq. (25) can be accurately obtained with the help of a computer and some algorithms [41,42]. It is worth noting that the truncation of the dimension of matrix $a_{k,\varepsilon}$ should ensure that the numerical calculation results are within the convergence accuracy. The corresponding numerical results will be discussed in detail in Sec. III.

B. The classical limit: $l_{k,\varepsilon} \rightarrow \infty$

In the semiclassical theory [10–14], the incident laser beam is described by the classical field, that is,

$$A_{k,\varepsilon}^{\text{cl}}(x) = \frac{\Lambda}{2} (\varepsilon e^{-ik \cdot x} + \varepsilon^* e^{ik \cdot x}). \quad (26)$$

Here, Λ is the classical field strength. The relationship [43] between the classical field strength and the density of photons in the field obeys

$$I = \frac{1}{2} \Lambda^2 \omega^2 = \frac{\omega l_{k,\varepsilon}}{V}, \quad (27)$$

where I is the laser intensity. Of course, we should follow the basic principle of quantum mechanics that quantum theory tends to be classical in the large quantum number limit. So in this section, we will use Eq. (27) to prove that the transition matrix element S_{fi} can reduce to the semiclassical result when $l_{k,\varepsilon} \rightarrow \infty$. In addition, for convenience, we omitted the subscript of $l_{k,\varepsilon}, n_{k,\varepsilon}, a_{k,\varepsilon}$, and $a_{k,\varepsilon}^\dagger$ in the proof.

First, M_N in Eq. (20) can be expanded as

$$M_N = \sum_{r=-2}^{+2} Y_r, \quad (28)$$

where

$$\begin{aligned} Y_0 &= \bar{u}_{p'S'} \not{\epsilon}' u_{pS} \langle n | S_{p'}^\dagger D_{p'} D_p^\dagger S_p | l \rangle + \frac{e^2 g^2 k \cdot \varepsilon'}{2k \cdot pk \cdot p'} \\ &\quad \times \langle n | S_{p'}^\dagger D_{p'} \bar{u}_{p'S'} (\not{\epsilon} \not{\epsilon}'^* a a^\dagger + \varepsilon'^* \not{k} \not{\epsilon} a^\dagger a) u_{pS} D_p^\dagger S_p | l \rangle, \end{aligned}$$

$$\begin{aligned}
Y_{-1} &= \frac{eg}{2} \bar{u}_{p's'} \left[\frac{\not{\epsilon}' \not{k} \not{k}}{k \cdot p} - \frac{\not{k} \not{k} \not{\epsilon}'}{k \cdot p'} \right] u_{ps} \langle n | S_p^\dagger D_{p'} a D_p^\dagger S_p | l \rangle, \\
Y_1 &= \frac{eg}{2} \bar{u}_{p's'} \left[\frac{\not{\epsilon}' \not{\epsilon}^* \not{k}}{k \cdot p} - \frac{\not{\epsilon}^* \not{k} \not{\epsilon}'}{k \cdot p'} \right] u_{ps} \langle n | S_p^\dagger D_{p'} a^\dagger D_p^\dagger S_p | l \rangle, \\
Y_{-2} &= \frac{e^2 g^2 k \cdot \epsilon' \cos \xi}{2k \cdot p k \cdot p'} \bar{u}_{p's'} \not{k} u_{ps} \langle n | S_p^\dagger D_{p'} a^2 D_p^\dagger S_p | l \rangle, \\
Y_2 &= \frac{e^2 g^2 k \cdot \epsilon' \cos \xi}{2k \cdot p k \cdot p'} \bar{u}_{p's'} \not{k} u_{ps} \langle n | S_p^\dagger D_{p'} a^\dagger a^\dagger D_p^\dagger S_p | l \rangle. \quad (29)
\end{aligned}$$

We may as well compute Y_0 first. When $l \rightarrow \infty$, there is

$$\lim_{\substack{l \rightarrow \infty \\ n \rightarrow \infty \\ N=l-n}} \langle n | S_p^\dagger D_{p'} D_p^\dagger S_p | l \rangle = \lim_{\substack{l \rightarrow \infty \\ n \rightarrow \infty \\ N=l-n}} \sum_{m=0} \langle n | S_p^\dagger D_{p'} | m \rangle \langle m | D_p^\dagger S_p | l \rangle. \quad (30)$$

Through the analysis, we find that only $m \rightarrow \infty$ contributes to Eq. (30). Due to [39]

$$\lim_{\substack{l \rightarrow \infty \\ m \rightarrow \infty}} \langle m | D_p^\dagger S_p | l \rangle = e^{i(l-m)\beta_1} \mathcal{F}_{m-l}(\zeta_1, \eta_1, \beta_1), \quad (31)$$

where

$$\begin{aligned}
\zeta_1 e^{i\beta_1} &= \lim_{m \rightarrow \infty} -2eg\sqrt{m} \frac{p \cdot \epsilon}{k \cdot p} = -e\Lambda \frac{p \cdot \epsilon}{k \cdot p}, \\
\eta_1 &= \lim_{l \rightarrow \infty} \frac{e^2 g^2 l}{2k \cdot p} \cos \xi = \frac{1}{2} \frac{e^2 \Lambda^2}{4k \cdot p} \cos \xi. \quad (32)
\end{aligned}$$

In the above formula, Eq. (27) is used. The function \mathcal{F}_j is defined as

$$\mathcal{F}_j(\zeta, \eta, \beta) = \sum_{l=-\infty}^{\infty} e^{-i2l\beta} J_{-j-2l}(\zeta) J_l(\eta), \quad (33)$$

and $J_{-j-2l}(\zeta)$, $J_l(\eta)$ represent the Bessel function.

Similarly,

$$\lim_{\substack{n \rightarrow \infty \\ m \rightarrow \infty}} \langle m | D_{p'}^\dagger S_p | n \rangle = e^{i(n-m)\beta_2} \mathcal{F}_{m-n}(\zeta_2, \eta_2, \beta_2), \quad (34)$$

and ζ_2 , η_2 , and β_2 are given by

$$\zeta_2 e^{i\beta_2} = -e\Lambda \frac{p' \cdot \epsilon}{k \cdot p'}, \quad \eta_2 = \frac{1}{2} \frac{e^2 \Lambda^2}{4k \cdot p'} \cos \xi. \quad (35)$$

Then, we have

$$\begin{aligned}
&\lim_{\substack{l \rightarrow \infty \\ n \rightarrow \infty \\ N=l-n}} \langle n | S_p^\dagger D_{p'} D_p^\dagger S_p | l \rangle \\
&= e^{iN\beta_1} \sum_{s_1} e^{is_1(\beta_2 - \beta_1)} \mathcal{F}_{s_1}^*(\zeta_2, \eta_2, \beta_2) \mathcal{F}_{s_1-N}(\zeta_1, \eta_1, \beta_1). \quad (36)
\end{aligned}$$

By Fourier series, $\mathcal{F}_j(\zeta, \eta, \beta)$ can be expressed as an integral,

$$\begin{aligned}
\mathcal{F}_j(\zeta, \eta, \beta) &= \int_{-\pi}^{\pi} \frac{dy}{2\pi} \exp[ijy + i\zeta \sin y \\
&\quad + i\eta \sin(2y - 2\beta)]. \quad (37)
\end{aligned}$$

Using the Poisson summation formula and Eq. (37), we obtain

$$\begin{aligned}
&\sum_{s_1} e^{is_1(\beta_2 - \beta_1)} \mathcal{F}_{s_1}^*(\zeta_2, \eta_2, \beta_2) \mathcal{F}_{s_1-N}(\zeta_1, \eta_1, \beta_1) \\
&= \int_{-\pi}^{\pi} \frac{d\theta_1}{2\pi} \exp[-iN\theta_1 - i\zeta_2 \sin(\theta_1 + \beta_2 - \beta_1) \\
&\quad + i\zeta_1 \sin \theta_1 + i(\eta_1 - \eta_2) \sin(2\theta_1 - 2\beta_1)]. \quad (38)
\end{aligned}$$

Also,

$$\begin{aligned}
&i\zeta_1 \sin \theta_1 - i\zeta_2 \sin(\theta_1 + \beta_2 - \beta_1) \\
&= \frac{1}{2} \left[e^{i\theta_1} e^{-i\beta_1} \left(e\Lambda \frac{p' \cdot \epsilon}{k \cdot p'} - e\Lambda \frac{p \cdot \epsilon}{k \cdot p} \right) - \text{c.c.} \right]. \quad (39)
\end{aligned}$$

If we let

$$\begin{aligned}
\zeta e^{i\alpha} &= e\Lambda \frac{p' \cdot \epsilon}{k \cdot p'} - e\Lambda \frac{p \cdot \epsilon}{k \cdot p}, \\
\eta &= \eta_1 - \eta_2, \quad (40)
\end{aligned}$$

there is

$$\lim_{\substack{l \rightarrow \infty \\ n \rightarrow \infty \\ N=l-n}} \langle n | S_p^\dagger D_{p'} D_p^\dagger S_p | l \rangle = e^{iN\alpha} \mathcal{F}_{-N}(\zeta, \eta, \alpha). \quad (41)$$

Finally, we have

$$Y_0 = e^{iN\alpha} \mathcal{F}_{-N}(\zeta, \eta, \alpha) \bar{u}_{p's'} \left[\not{\epsilon}' + \frac{e^2 \Lambda^2 k \cdot \epsilon'}{4k \cdot p k \cdot p'} \not{k} \right] u_{ps}. \quad (42)$$

In the same way, we can obtain, in turn,

$$\begin{aligned}
Y_{-1} &= e^{i(N-1)\alpha} \mathcal{F}_{-N+1}(\zeta, \eta, \alpha) \frac{e\Lambda}{4} \bar{u}_{p's'} \left[\frac{\not{\epsilon}' \not{k} \not{k}}{k \cdot p} - \frac{\not{k} \not{k} \not{\epsilon}'}{k \cdot p'} \right] u_{ps}, \\
Y_1 &= e^{i(N+1)\alpha} \mathcal{F}_{-N-1}(\zeta, \eta, \alpha) \frac{e\Lambda}{4} \bar{u}_{p's'} \left[\frac{\not{\epsilon}' \not{\epsilon}^* \not{k}}{k \cdot p} - \frac{\not{\epsilon}^* \not{k} \not{\epsilon}'}{k \cdot p'} \right] u_{ps}, \\
Y_{-2} &= e^{i(N-2)\alpha} \mathcal{F}_{-N+2}(\zeta, \eta, \alpha) \bar{u}_{p's'} \frac{e^2 \Lambda^2 k \cdot \epsilon' \cos \xi}{8k \cdot p k \cdot p'} \not{k} u_{ps}, \\
Y_2 &= e^{i(N+2)\alpha} \mathcal{F}_{-N-2}(\zeta, \eta, \alpha) \bar{u}_{p's'} \frac{e^2 \Lambda^2 k \cdot \epsilon' \cos \xi}{8k \cdot p k \cdot p'} \not{k} u_{ps}. \quad (43)
\end{aligned}$$

The results in Eqs. (42) and (43) above are perfectly in agreement with the corresponding results obtained by Brown and Kibble [10].

III. NUMERICAL RESULTS

In the previous discussion, we prove that $d\sigma_N/d\Omega_{k'}$ will reduce to the semiclassical value as $l_{k,\epsilon} \rightarrow \infty$. Furthermore, Eq. (27) means that we could keep I constant through changing $l_{k,\epsilon}$ and V . That is to say, for a given intensity I , the problem that how $d\sigma_N/d\Omega_{k'}$ is affected by $l_{k,\epsilon}$ could be solved. Next, we will take linearly polarized light (the polarization parameter $\xi = 0$) as an example to give some specific numerical results of scattering cross section. For convenience in later calculations, we will take the direction of \mathbf{k} as the Z-axis direction and abbreviate $d\sigma_N/d\Omega_{k'}$ as $d\sigma_N/d\Omega$.

We take the laser frequency $\omega = 1.54$ eV ($\lambda \approx 805$ nm) and the initial electron kinetic-energy $E_p = 0$. As shown in Fig. 2(a), laser intensity will affect the total scattering cross section corresponding to $N = 1$ in the classical light field.

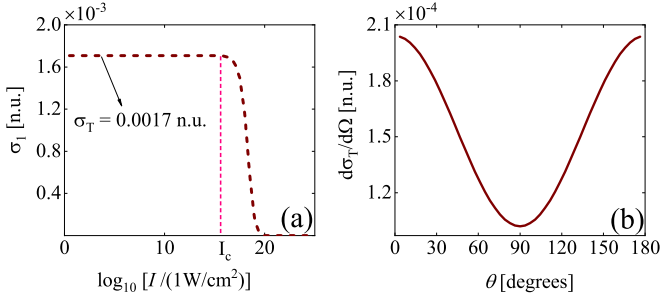


FIG. 2. Panel (a): the total scattering cross section in the classical light field for $N = 1$. Here, the initial electron kinetic-energy $E_p = 0$ and the abscissa is the logarithmic coordinate. Panel (b): the Thomson differential cross section.

Moreover, there is a critical strength: $I_c \approx 10^{16}$ W/cm², and it is the embodiment of the relativity effect [1]. Our calculations show that $d\sigma_1/d\Omega$ is invariant with intensity when $I \leq I_c$, and its value is exactly the Thomson differential cross-section $d\sigma_T/d\Omega$ [see Fig. 2(b)], that is, $\sigma_1 = \sigma_T = 8\pi r_e^2/3 = 0.0017$ n.u. Here, $r_e = e^2/(4\pi m)$ is the classical electron radius. Note that σ_T can be obtained by QED theory [44] wherein the corresponding physical image is a one-electron interacts with a single photon. However, according to our previous proof in Sec. II B, Fig. 2(a) is the result of a one-electron interacting with infinite photons ($l_{k,\varepsilon} \rightarrow \infty$). So it seems that σ_1 does not vary with $l_{k,\varepsilon}$ when I is constant.

Generally, the volume V is considered to be infinite in QED and the corresponding $j_{in} = 1/V \rightarrow 0$. However, Eq. (27) establishes the connection between the classical light field and the quantum light field, and it shows that single photon flux can have the corresponding classical intensity. Meanwhile, V is required to be larger than λ^3 in order that the field be a good approximation to a monochromatic plane wave [10]. This means that single-photon flux intensity is significant only if $I \leq \omega/\lambda^3 \approx 1.42 \times 10^4$ W/cm². Using Eq. (25), we calculate $d\sigma_1/d\Omega$ corresponding to different E_p s when $l_{k,\varepsilon} = 1$ and $V = \lambda^3$. The results are shown in Fig. 3. It can be seen that $d\sigma_1/d\Omega$ corresponding to $E_p = 0$ is just the Thomson differential cross section. This shows that Eq. (25) is reliable.

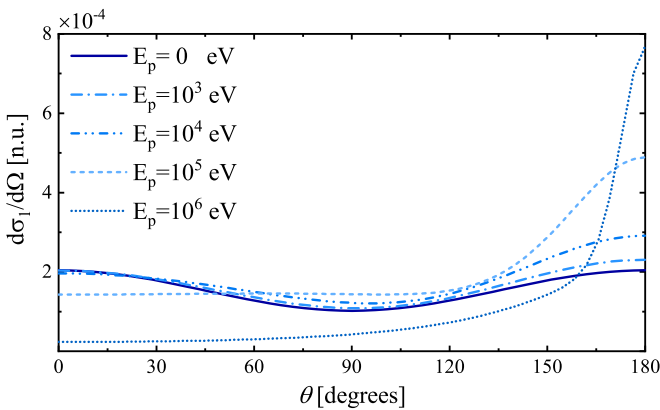


FIG. 3. Shows the differential cross sections for $l_{k,\varepsilon} = N = 1$. Here $\omega = 1.54$ eV and $V = \lambda^3$. In addition, our calculations indicate that these differential cross sections are independent of φ .

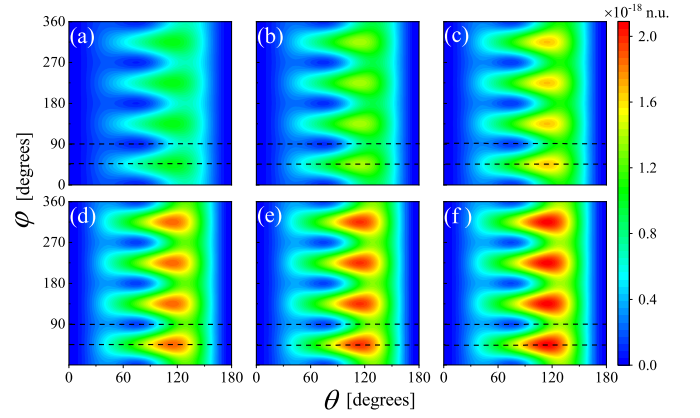


FIG. 4. The contour maps of $d\sigma_2/d\Omega$. Here, $\omega = 1.54$ eV and $I = 2\omega/\lambda^3$. Panels (a)–(e) correspond to $l_{k,\varepsilon} = 2, 3, 5, 10,$ and 20 , respectively. Panel (f): the semiclassical results.

Besides, we also find that these curves in Fig. 3 are consistent with corresponding semiclassical results and will not change with $l_{k,\varepsilon}$ for $I = \omega/\lambda^3$. The same is true for $I < \omega/\lambda^3$. Therefore, other than the scattered photon, the other $l_{k,\varepsilon} - 1$ photons have no contribution to $d\sigma_1/d\Omega$. However, the conclusion will be different for $d\sigma_2/d\Omega$.

Similarly, we can also compute $d\sigma_2/d\Omega$ under the prerequisite of ensuring $V \geq \lambda^3$. In this case, the significant intensity I must be less than $2\omega/\lambda^3$, namely, $I \leq 2.84 \times 10^4$ W/cm². In Fig. 4, we present contour maps of $d\sigma_2/d\Omega$ on the θ - φ plane when $I = 2\omega/\lambda^3$. We can see that $d\sigma_2/d\Omega$ is the periodic function of φ , and the period is $\pi/2$ rad. What is more important, $d\sigma_2/d\Omega$ can vary with $l_{k,\varepsilon}$. So to better understand this change, we give corresponding cross-sectional views of Fig. 4 when $\varphi = \pi/4$ and $\pi/2$ rad. The results are represented in Fig. 5. We find that with the increase in $l_{k,\varepsilon}$, $d\sigma_2/d\Omega$ also increases and approaches to the semiclassical value. Ulteriorly, we define the following parameter:

$$r_{\max} = \max \left[\frac{d\sigma_2}{d\Omega} \right]_l / \max \left[\frac{d\sigma_2}{d\Omega} \right]_c, \quad (44)$$

where $\max[\frac{d\sigma_2}{d\Omega}]_l$ is the maximum of $d\sigma_2/d\Omega$ when the initial photon number is $l_{k,\varepsilon}$, and $\max[\frac{d\sigma_2}{d\Omega}]_c$ represents the maximum value of the semiclassical results. As shown in Fig. 6, r_{\max} is already very close to 1.0 when $l_{k,\varepsilon} = 200$. However, the laser beam in the laboratory generally contains a large number of

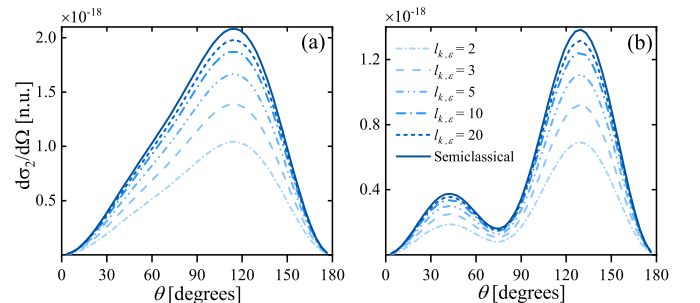


FIG. 5. The cross-sectional views corresponding to the black dotted lines in Fig. 4. Here, (a) $\varphi = \pi/4$ rad; (b) $\varphi = \pi/2$ rad.

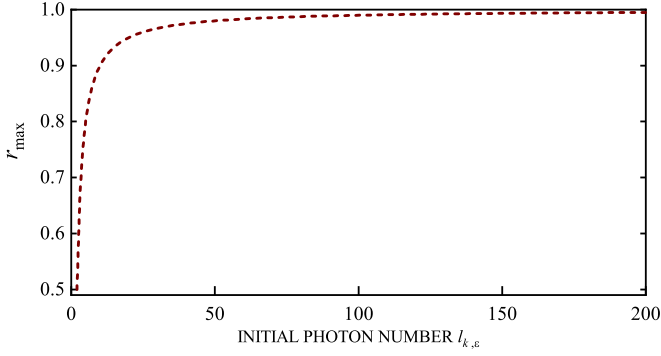


FIG. 6. The transition behavior of $d\sigma_2/d\Omega$ from quantum to semiclassical. The parameters ω and I are consistent with those in Fig. 4.

photons ($l_{k,\epsilon} > 10^5$). So it is difficult to observe the fluctuation of $d\sigma_2/d\Omega$ with $l_{k,\epsilon}$. In addition, our calculations show that the above conclusions are also applicable to $I < 2\omega/\lambda^3$.

IV. SUMMARY AND DISCUSSION

We take the solution of the Dirac equation containing the quantized light field as the initial and final states of entire scattering system in this paper. With keeping the intensity $I = \omega l_{k,\epsilon}/V$ constant, we numerically calculated the differential scattering cross sections corresponding to different $l_{k,\epsilon}$ s. The results show that within the effective intensity, $d\sigma_1/d\Omega$ will not be affected by $l_{k,\epsilon}$, but $d\sigma_2/d\Omega$ will increase with $l_{k,\epsilon}$ and quickly approach the semiclassical value. Although the fluctuation of $d\sigma_2/d\Omega$ does exist, its value is too small. If high-energy photons ($\omega \sim 10^4$ eV) are used, the order of magnitude of $d\sigma_2/d\Omega$ will be significantly increased to 10^{-10} n.u., and it may bring convenience to experimental detection. Moreover, in the large photon number limit ($l_{k,\epsilon} \rightarrow \infty$), we also prove that the transition matrix element S_{fi} obtained by using quantum electrodynamics to deal with multiphoton Compton scattering is consistent with that by the semiclassical theory.

It is worth noting that the above discussion is based on the fact that the initial state of the external field is the Fock state $|l_{k,\epsilon}\rangle$. However, strictly speaking, the incident laser beam should be described as the coherent state [45],

$$|Q\rangle = e^{-(1/2)|Q|^2} \sum_{L_{k,\epsilon}=0}^{\infty} \frac{Q^{L_{k,\epsilon}}}{\sqrt{L_{k,\epsilon}!}} |L_{k,\epsilon}\rangle, \quad (45)$$

where $Q = \sqrt{l_{k,\epsilon}}$ and $l_{k,\epsilon}$ represents the mean photon number of the incident laser beam. The Fock state $|L_{k,\epsilon}\rangle$ component in $|Q\rangle$ follows Poisson distribution:

$$P(L_{k,\epsilon}) = \frac{Q^{2L_{k,\epsilon}}}{L_{k,\epsilon}!} e^{-Q^2}. \quad (46)$$

Similar to the previous derivation in Sec. II A, we can easily get

$$[w_N]_{\text{coh}} = \sum_{L_{k,\epsilon}=N}^{\infty} P(L_{k,\epsilon}) [w_N]_{L_{k,\epsilon}}, \quad (47)$$

where $[w_N]_{\text{coh}}$ is the transition probability with the absorption of N photons when the initial state of the external field is the coherent state $|Q\rangle$. $[w_N]_{L_{k,\epsilon}}$ represents w_N corresponding to Fock state $|L_{k,\epsilon}\rangle$ and it can be obtained from Eq. (23). According to Eq. (47), we can obtain the differential scattering cross-section $[d\sigma_N/d\Omega]_{\text{coh}}$ corresponding to $|Q\rangle$.

At present, our calculation data show that when $\omega = 1.54$ eV and I is relatively small ($I \sim 10^4 - 10^7$ W/cm²), $[d\sigma_N/d\Omega]_{\text{coh}}$ will not change with $l_{k,\epsilon}$. However, For larger I , the corresponding $l_{k,\epsilon}$ is very large. In this case, our numerical calculation method will be difficult to carry out because $a_{k,\epsilon}$ and $a_{k,\epsilon}^\dagger$ lie on the e index in operators D_q^\dagger and S_q . Therefore, in a strong field with extremely high intensity, how $l_{k,\epsilon}$ affects the Compton scattering process is very worth exploring.

Finally, it should be pointed out that laser pulses used in real experiments are not single mode. Through Fourier decomposition, we can get the frequency spectrum of laser pulses, which characterize the space-time distribution of the laser pulse. Therefore, the interaction between electrons and laser pulses is actually equivalent to the interaction between the electron and the multimode quantum light field. This situation will be extremely complex and has greatly exceeded the scope of our paper. However, for laser pulses with a narrow frequency spectrum, our single-mode calculation results are still credible.

ACKNOWLEDGMENTS

This work was supported by the National Natural Science Foundation of China (NSFC) (Grants No. 11725417, No. 12088101, and No. U1930403) and Science Challenge Project (Grant No. TZ2018005).

APPENDIX A: THE PECIFIC EXPRESSION OF u_{qs}

In Sec. II A, we define

$$u_{qs} = \mathcal{P}(\mathcal{S} + s)v, \quad (A1)$$

where [39]

$$\mathcal{P} = \frac{(\not{q} + m_e)\not{k}}{2k \cdot q}, \quad (A2)$$

and

$$\mathcal{S} = \not{\epsilon}^* \not{\epsilon} + 1 = \sin \xi \begin{pmatrix} 1 & 0 & 0 & 0 \\ 0 & -1 & 0 & 0 \\ 0 & 0 & 1 & 0 \\ 0 & 0 & 0 & -1 \end{pmatrix}. \quad (A3)$$

Obviously, we have

$$\mathcal{S} \begin{pmatrix} x_1 \\ 0 \\ x_2 \\ 0 \end{pmatrix} = \sin \xi \begin{pmatrix} x_1 \\ 0 \\ x_2 \\ 0 \end{pmatrix}, \quad (A4)$$

and

$$\mathcal{S} \begin{pmatrix} 0 \\ y_1 \\ 0 \\ y_2 \end{pmatrix} = -\sin \xi \begin{pmatrix} 0 \\ y_1 \\ 0 \\ y_2 \end{pmatrix}. \quad (A5)$$

Here, x_1 , x_2 , y_1 , and y_2 are arbitrary complex numbers. Furthermore, there is also

$$\mathcal{S}(\mathcal{S} \pm \sin \xi)v = \pm \sin \xi (\mathcal{S} \pm \sin \xi)v. \quad (\text{A6})$$

Because v is an arbitrary bispinor, we might as well set $x_1 = y_1 = 1$ and $x_2 = y_2 = 0$. In this way, considering the normalization, we obtain

$$u_{q,s=+\sin \xi} = \sqrt{\frac{k \cdot q}{m_e \omega}} \frac{(\not{q} + m_e)\not{k}}{2k \cdot q} \begin{pmatrix} 1 \\ 0 \\ 0 \\ 0 \end{pmatrix}, \quad (\text{A7})$$

and

$$u_{q,s=-\sin \xi} = \sqrt{\frac{k \cdot q}{m_e \omega}} \frac{(\not{q} + m_e)\not{k}}{2k \cdot q} \begin{pmatrix} 0 \\ 1 \\ 0 \\ 0 \end{pmatrix}. \quad (\text{A8})$$

Then, it is easy to obtain

$$u_{qs}^\dagger u_{qs'} = \frac{q^0}{m_e} \delta_{ss'}, \quad (\text{A9})$$

$$\sum_s u_{qs} \bar{u}_{qs} = \frac{\not{q} + m_e}{2m_e}. \quad (\text{A10})$$

APPENDIX B: BOUNDARY TREATMENT OF $\psi_{qn's}^V(x)$

We note that $\psi_{qn',k,\varepsilon,s}^V(x)$ could not reduce to $e^{-iE_q t} \langle \mathbf{r} | q \rangle \otimes | n'_{k,\varepsilon} \rangle$ as $t \rightarrow \pm\infty$ although it satisfies Eq. (12). In fact, for an actual Compton scattering system, we must consider the coupling and decoupling processes between the electrons and the light field. To this end, we introduce a slowly varying function,

$$F(t) = \lim_{\Gamma \rightarrow 0^+} \begin{cases} e^{-\Gamma t}, & t > 0 \\ e^{\Gamma t}, & t \leq 0 \end{cases}. \quad (\text{B1})$$

Correspondingly,

$$H_0 \rightarrow H_0 = \gamma^0 \boldsymbol{\gamma} \cdot [-i\nabla + eF(t)\mathbf{A}_{k,\varepsilon}(x)] + \gamma^0 m_e. \quad (\text{B2})$$

With the help of $\frac{\partial F(t)}{\partial t} \rightarrow 0$, it is not hard to prove that $\psi_{qn',k,\varepsilon,s}^V(x)$ is still the solution of Eq. (12) by only replacing g in Eq. (13) with $gF(t)$. As a result, $\psi_{qn',k,\varepsilon,s}^V(x)$ will adiabatically tend to the free state $e^{-iE_q t} \langle \mathbf{r} | q \rangle \otimes | n'_{k,\varepsilon} \rangle$ as $t \rightarrow \pm\infty$.

-
- [1] F. Ehlötzky, K. Krajewska, and J. Z. Kamiński, Fundamental processes of quantum electrodynamics in laser fields of relativistic power, *Rep. Prog. Phys.* **72**, 046401 (2009).
- [2] A. Di Piazza, C. Müller, K. Z. Hatsagortsyan, and C. H. Keitel, Extremely high-intensity laser interactions with fundamental quantum systems, *Rev. Mod. Phys.* **84**, 1177 (2012).
- [3] T. Blackburn, Radiation reaction in electron–beam interactions with high-intensity lasers, *Rev. Mod. Plasma Phys.* **4**, 5 (2020).
- [4] A. Gonoskov, T. Blackburn, M. Marklund, and S. Bulanov, Charged particle motion and radiation in strong electromagnetic fields, [arXiv:2107.02161](https://arxiv.org/abs/2107.02161).
- [5] N. D. Sengupta, On the scattering of electromagnetic waves by free electron. I. Classical theory, *Bull. Calcutta Math. Soc.* **41**, 187 (1949).
- [6] E. S. Sarachik and G. T. Schappert, Classical theory of the scattering of intense laser radiation by free electrons, *Phys. Rev. D* **1**, 2738 (1970).
- [7] Y. I. Salamin and F. H. M. Faisal, Harmonic generation by superintense light scattering from relativistic electrons, *Phys. Rev. A* **54**, 4383 (1996).
- [8] E. Esarey, S. K. Ride, and P. Sprangle, Nonlinear thomson scattering of intense laser pulses from beams and plasmas, *Phys. Rev. E* **48**, 3003 (1993).
- [9] A. Nikishov and V. Ritus, Quantum processes in the field of a plane electromagnetic wave and in a constant field. i, *Sov. Phys. JETP* **19**, 529 (1964).
- [10] L. S. Brown and T. W. B. Kibble, Interaction of intense laser beams with electrons, *Phys. Rev.* **133**, A705 (1964).
- [11] I. Goldman, Intensity effects in compton scattering, *Phys. Lett.* **8**, 103 (1964).
- [12] P. Panek, J. Z. Kamiński, and F. Ehlötzky, Laser-induced compton scattering at relativistically high radiation powers, *Phys. Rev. A* **65**, 022712 (2002).
- [13] C. Harvey, T. Heinzl, and A. Ilderton, Signatures of high-intensity compton scattering, *Phys. Rev. A* **79**, 063407 (2009).
- [14] D. Seipt and B. Kämpfer, Nonlinear compton scattering of ultrashort intense laser pulses, *Phys. Rev. A* **83**, 022101 (2011).
- [15] G. Mourou, Nobel lecture: Extreme light physics and application, *Rev. Mod. Phys.* **91**, 030501 (2019).
- [16] T. J. Englert and E. A. Rinehart, Second-harmonic photons from the interaction of free electrons with intense laser radiation, *Phys. Rev. A* **28**, 1539 (1983).
- [17] C. Bula, K. T. McDonald, E. J. Prebys, C. Bamber, S. Boege, T. Kotseroglou, A. C. Melissinos, D. D. Meyerhofer, W. Ragg, D. L. Burke, R. C. Field, G. Horton-Smith, A. C. Odian, J. E. Spencer, D. Walz, S. C. Berridge, W. M. Bugg, K. Shmakov, and A. W. Weidemann, Observation of Nonlinear Effects in Compton Scattering, *Phys. Rev. Lett.* **76**, 3116 (1996).
- [18] S.-y. Chen, A. Maksimchuk, and D. Umstadter, Experimental observation of nonlinear thomson scattering, *Nature (London)* **396**, 653 (1998).
- [19] M. Babzien, I. Ben-Zvi, K. Kusche, I. V. Pavlishin, I. V. Pogorelsky, D. P. Siddons, V. Yakimenko, D. Cline, F. Zhou, T. Hirose, Y. Kamiya, T. Kumita, T. Omori, J. Urakawa, and K. Yokoya, Observation of the Second Harmonic in Thomson Scattering from Relativistic Electrons, *Phys. Rev. Lett.* **96**, 054802 (2006).
- [20] W. Yan, C. Fruhling, G. Golovin, D. Haden, J. Luo, P. Zhang, B. Zhao, J. Zhang, C. Liu, M. Chen, S. Chen, S. Banerjee, and D. Umstadter, High-order multiphoton thomson scattering, *Nat. Photonics* **11**, 514 (2017).
- [21] C. I. Moore, J. P. Knauer, and D. D. Meyerhofer, Observation of the Transition from Thomson to Compton Scattering in Multiphoton Interactions with Low-Energy Electrons, *Phys. Rev. Lett.* **74**, 2439 (1995).

- [22] D. D. Meyerhofer, J. P. Knauer, S. J. McNaught, and C. I. Moore, Observation of relativistic mass shift effects during high-intensity laser–electron interactions, *J. Opt. Soc. Am. B* **13**, 113 (1996).
- [23] I. A. Ivanov and K. T. Kim, Atomic ionization driven by the quantized electromagnetic field in a fock state, *Phys. Rev. A* **102**, 023117 (2020).
- [24] L. Keldysh, Ionization in field of a strong electromagnetic wave, *JETP* **20**, 1307 (1964).
- [25] F. H. M. Faisal, Multiple absorption of laser photons by atoms, *J. Phys. B* **6**, L89 (1973).
- [26] H. R. Reiss, Effect of an intense electromagnetic field on a weakly bound system, *Phys. Rev. A* **22**, 1786 (1980).
- [27] A. Gombkötő, A. Czirják, S. Varró, and P. Földi, Quantum-optical model for the dynamics of high-order-harmonic generation, *Phys. Rev. A* **94**, 013853 (2016).
- [28] A. Gombkötő, P. Földi, and S. Varró, Quantum-optical description of photon statistics and cross correlations in high-order harmonic generation, *Phys. Rev. A* **104**, 033703 (2021).
- [29] D. Seipt, T. Heinzl, M. Marklund, and S. S. Bulanov, Depletion of Intense Fields, *Phys. Rev. Lett.* **118**, 154803 (2017).
- [30] A. Ilderton and D. Seipt, Backreaction on background fields: A coherent state approach, *Phys. Rev. D* **97**, 016007 (2018).
- [31] D.-J. Dai and L.-B. Fu, Quantum fluctuations in strong field ionization, *Europhys. Lett.* **135**, 23001 (2021).
- [32] D. Wolkow, Über eine klasse von lösungen der diracschen gleichung, *Z. Phys.* **94**, 250 (1935).
- [33] W. H. Furry, On bound states and scattering in positron theory, *Phys. Rev.* **81**, 115 (1951).
- [34] Z. Fried and J. H. Eberly, Scattering of a high-intensity, low-frequency electromagnetic wave by an unbound electron, *Phys. Rev.* **136**, B871 (1964).
- [35] J. H. Eberly and H. R. Reiss, Electron self-energy in intense plane-wave field, *Phys. Rev.* **145**, 1035 (1966).
- [36] F. F. Körmendi and G. Farkas, Quantum electrodynamics of strong-field compton scattering and its ponderomotive and drift energies, *Phys. Rev. A* **59**, 4172 (1999).
- [37] J. Bergou and S. Varro, Nonlinear scattering processes in the presence of a quantised radiation field. II. relativistic treatment, *J. Phys. A* **14**, 2281 (1981).
- [38] P. Filipowicz, Relativistic electron in a quantised plane wave, *J. Phys. A* **18**, 1675 (1985).
- [39] D. S. Guo and T. Aberg, Quantum electrodynamical approach to multiphoton ionisation in the high-intensity h field, *J. Phys. A* **21**, 4577 (1988).
- [40] D. S. Guo and T. Aberg, Orthogonality and completeness of the quantum electrodynamical volkov solutions, *J. Phys. B: At., Mol. Opt. Phys.* **24**, 349 (1991).
- [41] N. J. Higham, The scaling and squaring method for the matrix exponential revisited, *SIAM J. Matrix Anal. Appl.* **26**, 1179 (2005).
- [42] A. H. Al-Mohy and N. J. Higham, A new scaling and squaring algorithm for the matrix exponential, *SIAM J. Matrix Anal. Appl.* **31**, 970 (2010).
- [43] M. Mittleman, *Introduction to the Theory of Laser-Atom Interactions* (Plenum, New York, 1993).
- [44] M. E. Peskin, *An Introduction To Quantum Field Theory* (CRC, Boca Raton, FL, 2018).
- [45] R. J. Glauber, Coherent and incoherent states of the radiation field, *Phys. Rev.* **131**, 2766 (1963).